Supporting Information for

Irreversible Topological Transition of a Stretched Superhelix: The Interplay of Chiralities

Saeed Najafi*
Department of Chemical and Biomolecular Engineering, University of Pennsylvania, Philadelphia, PA 19104, United States

MODEL

The superhelix monomers are connected to their first neighbors by means of stiff bonds. The only non-bonded interaction to which the monomers are subject is a short-ranged excluded volume, enforcing steric hindrance and preventing the chain from the self crossing. This standard model of the polymers is then provided with bending and torsion potentials, whose reference angles are parametrized based on a native structure. We use the standard Kremer-Grest model of chains [1, 2]. The superhelix chain is described as a collection of identical monomers, connected by FENE bonds [3]. The only non-bonded interaction among the monomers is a purely repulsive Weeks-Chandler-Anderson (WCA) [4] potential. Triplets and quadruplets of subsequent monomers interact *via* bending and torsion potentials, respectively.

The total potential energy of the system is:

$$\mathcal{V} = U_{\rm WCA} + U_{\rm FENE} + U_{\rm bending} + U_{\rm torsion} \qquad (1)$$

The WCA potential is given by:

$$U_{\rm WCA} = \frac{1}{2}\sum_{(i,j),j\neq i}^{N} V(d_{i,j})$$
$$V(r) = \begin{cases} 4\epsilon\left[\left(\frac{\sigma}{r}\right)^{12} - \left(\frac{\sigma}{r}\right)^{6} + \frac{1}{4}\right] & \text{for } r \le 2^{1/6}\sigma \\ 0 \quad \text{otherwise} \end{cases} \qquad (2)$$

and the FENE potential reads:

$$U_{\rm FENE} = -\sum_{i=0}^{N-2} \frac{\kappa_{fene}}{2}\left(\frac{R_0}{\sigma}\right)^2 \ln\left[1 - \left(\frac{d_{i,i+1}}{R_0}\right)^2\right] \qquad (3)$$

where $d_{i,i+1} = |\vec{r}_i - \vec{r}_{i+1}|$ is the distance of the monomer centers i and $i+1$, R_0 is the maximum bond length and κ_{fene} is the FENE interaction strength. Note that the diameter σ of the monomer is taken as the length unit, and corresponds to the separation between two consecutive monomers; all distances are expressed in reduced units. The WCA strength ϵ is taken as the energy unit, and the FENE bond constant κ_{fene} was set to 30ϵ as it is customary for the Kremer-Grest model [1, 2].

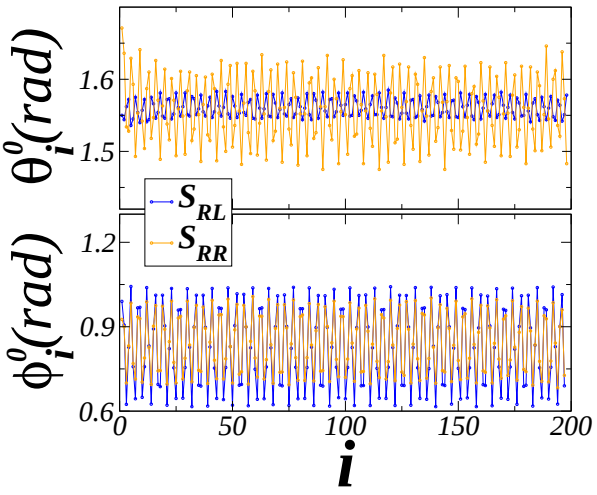

FIG. 1. In this plot we show the distribution of the intermolecular bending (θ_i^0) and torsional (ϕ_i^0) angles of the superhelixes in their native state for $\kappa_{bend} = \kappa_{tor} = 100k_BT$, where i is the index of the monomers of the superhelix.

The bending and torsion potentials are:

$$U_{\rm bending} = \sum_{i=1}^{N-2} \kappa_{bend}(\theta_i - \theta_i^0)^2$$
$$U_{\rm torsion} = \sum_{i=1}^{N-3} U_i^{tor} \qquad (4)$$

with:

$$U_i^{tor} = \kappa_{tor}\left(\cos(\phi_i - \phi_i^0) + \frac{1}{3}\cos(3(\phi_i - \phi_i^0))\right)$$

θ_i^0 and ϕ_i^0 are the bending and torsion angle of the i-th monomer in the native states, respectively. κ_{bend} and κ_{tor} are the corresponding bending and torsion stiffness, respectively.

In Fig. 3, we show the distribution of the bending (θ_i^0) and torsional (ϕ_i^0) angles of the superhelixes in their native sate. As it is evident from plot, the S_{RR} posses a broader distribution of θ_i^0 in compare to the S_{RL}, while the opposite trend is weakly observed as for ϕ_i^0. This feature of the superhelixes reveals their statics due to the topology in the native state, which barely manifest itself in the intermolecular bending and torsion angles. Similarly, in Fig. 2, we show the bending (θ_i^S) and tor-

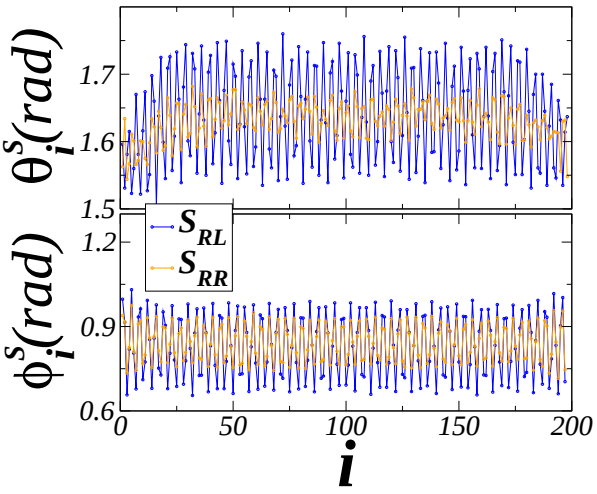

FIG. 2. In this plot we show the distribution of the intermolecular bending (θ_i^S) and torsional (ϕ_i^S) angles of the superhelixes in the stretched state, where i is the index of the monomers of the superhelix (in this plot the S_{RR} after stretching switch its topology to S_{RL}), with having set $\kappa_{bend} = \kappa_{tor} = 100 k_B T$ and $d = 70\sigma$.

sional (ϕ_i^S) angles of the superhelixes in the stretched state of the superhelixes. The angles of the stretched S_{RR} is shown after the topology transition when the superhelix is equilibrated. Interestingly, the opposite trend of the bending angles in the native state is observed in the stretched state.

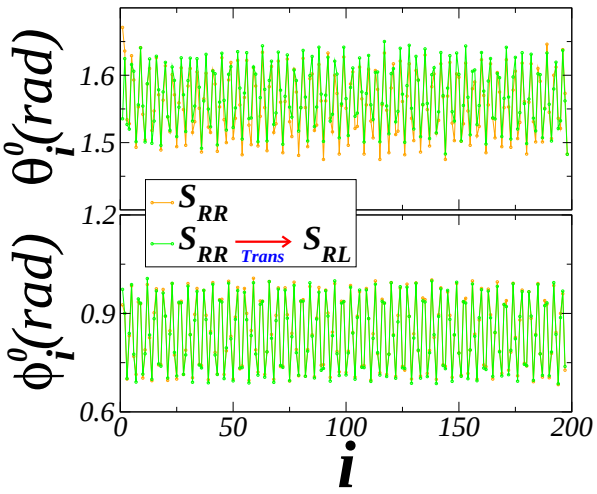

FIG. 3. In this plot we show the distribution of the intermolecular bending (θ_i^0) and torsional (ϕ_i^0) angles of the S_{RR} in the un-stretched state before and after the topology transition at $\kappa_{bend} = \kappa_{tor} = 100 k_B T$, where i is the index of the monomers of the superhelix.

SIMULATION METHOD

The potential of Eq. 1 is employed to perform overdamped Molecular Dynamics simulations in implicit solvent by means of the following Langevin equations of motion:

$$-\frac{\partial \mathcal{V}_i}{\partial \vec{r}_i(t)} - m\gamma \vec{v}_i(t) + \vec{R}(t) = 0 \qquad (5)$$

where m, v_i, $\mathcal{V}_i$, γ, R_i and r_i are the mass, velocity, local potential energy, friction coefficient, random force and coordinate of the i-th monomer, respectively. The equations of motion of the system are integrated with a symplectic, first order algorithm [5]. The system parameters are listed in Table I.

In order to investigate how the stretching of the superhelixes along the $z-axis$ affect the superhelix's topology we performed different sets of simulations. We stretched the end of the superhelix by applying a constant force to $\{0, 0, d\}$ while the other end is fixed at $\{0, 0, 0\}$ without clamping. For each d of the superhelixes, we ran 40 independent simulations to characterize and quantify the topology transition. A single simulation runs according to the following steps:

1. The superhelixes with the uniform elasticity and identical radius $\sim 3.4\sigma$ (with 200 monomers) are initialized and equilibrated in the native state, at which the ends of the superhelixes are fixed without clamping at $\{0, 0, 0\}$ and $\{0, 0, 8.6\sigma\}$.

2. We fix one end of the superhelix and stretch the other end to $\{0, 0, d\}$, with an appropriate stretching force, which does not affect the helical structure of the superhelix chains while ensuring that the stretched end of the superhelix has reached $\{0, 0, d\}$.

3. We run the simulations long enough such that the stretched superhelixes reach the equilibrium state and feature a plateau of the potential energy landscape.

As for the release, we take the final configuration of the equilibrated stretched superhelix and set the z component of the stretching force equal to *zero*, and let the superhelix to relax and reach the native bending and torsional angles.

TOPOLOGY ANALYSIS

The topological state of the superhelixes have been characterized using the the writhe of the coarse grained chains [6], which is a descriptor of the net sign of the superhelixes chirality:

Parameter	Value
m	1
ϵ	1
MD time unit $\tau_{MD} = \sigma\sqrt{\frac{m}{\epsilon}}$	1
$\Delta t\ [\tau_{MD}]$	$2 \cdot 10^{-3}$
$R_0\ [\sigma]$	1.5
$\kappa_{fene}\ [\epsilon]$	30
$\tau_{fricl}\ [\tau_{MD}]$	1
$T\ [\frac{\epsilon}{k_B}]$	0.1

TABLE I. System parameters.

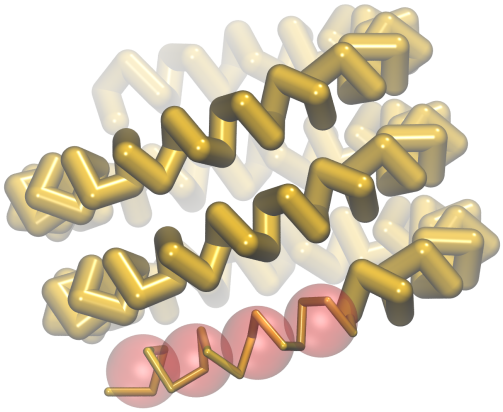

FIG. 4. The transparent red spheres show the center mass of the every 4 consecutive monomers of the superhelix. The total number of the coarse grained monomers of the superhelix with 200 monomers that are used to calculate the Wr, is $N_c = 50$.

$$Wr = 2\sum_{i=2}^{N_c}\sum_{i<j}\frac{\Omega_{ij}}{4\pi}, \tag{6}$$

where $\Omega_{ij}/4\pi$ is the Gauss integral along the coarse grained segments i, j and N_c is the total number of coarse grained segments of the superhelix monomers. For $Wr < 0$ and $Wr > 0$, the net chirality of the superhelix is left and right-handed, respectively. The coarse grained chain is basically identified as the collection of the center mass of every 4 consecutive monomers of the superhelixes, as shown in Fig. 3. In our analysis, we take into account the fact that the topology change of the superhelixes is independent of the helix chirality, *i.e.* during the topology transition the chirality of the helix remains unchanged. In order to ascertain the chirality transition of the stretched superhelix, we simultaneously quantify the total potential energy of the superhelixes; at the end of transition the stretched superhelix reaches a equilibrium state with constant conformational energy.

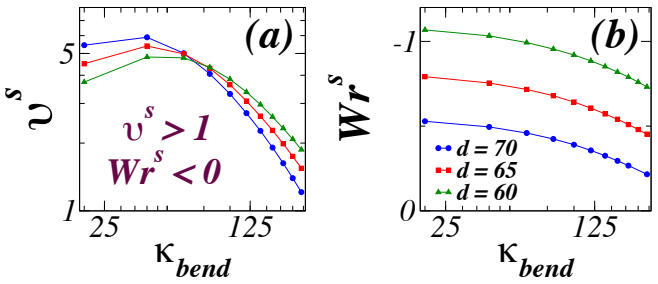

FIG. 5. Plot (a) and (b) indicate υ and Wr of the S_{RL} in the equilibrated stretched state as a function of κ_{bend} for $\frac{d}{\sigma} = 70,\ 65,\ 60$ at $\kappa_{tor} = 100k_BT$. As it shown in plots, we invariably have : $\upsilon^s > 1$ and $Wr^S < 0$ (with no topology transition).

THE STRETCHED S_{RL}

In Fig. 5, we show the υ^s of the stretched S_{RL} as a function of κ_{bend}, at $d = 70$ and $\kappa_{tor} = 100k_BT$. As it is shown in the plot, for every value of the bending stiffness the υ^s is larger than 1, which implies that the torsion induced strain of the superhelix is smaller than the bending induces tension, which has a component perpendicular to the stretching plane. This characteristic of the S_{RL} due to its topology, give rise to substantially lower conformational energy of the stretched superhelix in compare to the S_{RR} in the regime where the topology transition can not occur at the same κ_{bend}, κ_{tor} and d values. We should mention that after the topology transition, the released superhelix at equilibrium (with topology of the S_{RL}), still has the tilted conformation in relative to the z-axis due to its forcefield and more importantly, stretching the superhelix once agin does not give rise to topology transition..

* snajafi@seas.upenn.edu

[1] G. S. Grest and K. Kremer, Phys. Rev. A **33**, 3628 (1986).
[2] K. Kremer and G. S. Grest, The Journal of Chemical Physics **92**, 5057 (1990).
[3] M. Bishop, M. H. Kalos, and H. L. Frisch, The Journal of Chemical Physics **70**, 1299 (1979).
[4] J. D. Weeks, D. Chandler, and H. C. Andersen, The Journal of Chemical Physics **54**, 5237 (1971).
[5] D. C. Rapaport, *The Art of Molecular Dynamics Simulation*, 2nd ed. (Cambridge University Press, 2004).
[6] K. Klenin and J. Langowski, Biopolymers **54**, 307 (2000).